MR Angiography of Spinal Vascular Malformations

Mario Mascalchi, Maria Cristina Bianchi, Nello Quilici, Salvatore Mangiafico, Giampiero Ferrito, Riccardo Padolecchia, and Carlo Bartolozzi

PURPOSE: To determine the potential and limitations of MR angiography in the evaluation of spinal vascular malformations. **METHODS:** Eleven consecutive patients with spinal vascular malformations proved with spinal selective arteriography underwent two-dimensional phase-contrast MR angiography. **RESULTS:** Abnormal vessels within the spinal canal were identified with MR angiography in 10 patients. In 1 patient with a dural arteriovenous fistula no definite vascular abnormality was seen with MR angiography. Correlation of MR angiography with spinal selective arteriography showed that the former allowed identification of the arterial feeder in 3 patients with intramedullary arteriovenous malformations and 2 with perimedullary arteriovenous fistula, whereas the source of intradural draining vein was seen in only 2 of 6 patients with dural arteriovenous fistula. **CONCLUSION:** MR angiography is a promising complementary tool to MR imaging for detection and characterization of spinal vascular malformations.

Index terms: Arteriovenous malformations, spinal; Spine, magnetic resonance; Magnetic resonance angiography

AJNR Am J Neuroradiol 16:289–297, February 1995

Selective spinal arteriography is the primary imaging method for diagnosis, classification, treatment, and follow-up of spinal vascular malformations (1). These are uncommon disorders and include intramedullary arteriovenous malformations, perimedullary arteriovenous fistulas, and dural arteriovenous fistulas (1, 2). Selective spinal arteriography requires considerable technical skills, is time consuming because all spinal vascular pedicles have to be catheterized, exposes the patient and the operator to a high radiation dose, and is not without risk. Hence selective spinal arteriography is not suitable as a screening modality for spinal vascular malformations. Until now, myelography, computed tomography (CT) after myelography, and magnetic resonance (MR) imaging have been used to select patients for selective spinal arteriography.

Received February 2, 1994; accepted after revision July 5.

From the Cattedra di Radiologia, Universita' di Pisa (M.M., C.B.), Unita' Operativa Neuroradiologia, Ospedale S. Chiara (M.C.B., R.P.), Pisa; Unita' Operativa Neuroradiologia, Spedali Riuniti (N.Q., G.F.), Livorno; and Unita Operativa Neuroradiologia, Ospedale di Careggi (S.M.), Firenze; Italy.

Address reprint requests to Mario Mascalchi, MD, PhD, Cattedra di Radiologia, Universita' di Pisa, Via Roma 67, 56126 Pisa, Italy.

AJNR 16:289–297, Feb 1995 0195-6108/95/1602–0289
© American Society of Neuroradiology

MR angiography is a noninvasive modality now widely used for intracranial vascular disorders (3). In comparison, scanty data are available on the potential and limitations of MR angiography for spinal vascular disorders (2, 4, 5). We report MR angiography findings in a series of patients with spinal vascular malformations proven with selective spinal arteriography.

Patients and Methods

From April 1992 to December 1993, 11 consecutive patients with native (n = 10) or recurrent (n = 1) spinal vascular malformations proved with selective spinal arteriography underwent MR angiography at one MR center. Clinical features and results of MR imaging, myelography, CT after myelography, and selective spinal arteriography studies are reported in Table 1. Follow-up MR angiography studies after treatment of the spinal vascular malformation were obtained in three cases. To define the normal appearance of the spine on MR angiography, seven healthy volunteers were examined with the same technique and protocol reported below.

MR Angiography Examination Protocol

All MR angiography studies were done on a 0.5-T MR unit with 7.7 mT/m maximum gradient capability using two-dimensional phase contrast technique (6). In 10 patients with thoracic lesions a circularly polarized surface

TABLE 1: Clinical features and MR, myelography, and selective spinal arteriography findings in 11 patients with spinal vascular malformations

Case	Sex/Age, y	Clinical Features (age of onset, y)	MR Imaging	Myelography, CT Myelography	Selective Spinal Arteriography
1	F/25	Paresthesias to the lower limbs (20)	Intramedullary and perimedullary areas of signal void	np	Intramedullary AVM (glomus type) fed by L T-10 artery; anterior and posterior descending and ascending venous drainage
2	M/20	Left arm paresthesia and mild paresis (20)	Intramedullary area of signal void; increased signal of the spinal cord on proton-density and T2-weighted images	np	Intramedullary AVM (glomus type) fed by left cervical ascending artery; anterior ascending venous drainage
3	F/40	Radicular pain in the right abdomen and paraparesis (19)	Intramedullary area of signal void	np	Intramedullary AVM (juvenile type) fed by L and R T-5 and L T-8 arteries; ascending and descending posterior venous drainage
4	M/37	Paresthesias to the lower limbs and paraparesis (36)	Perimedullary areas of signal void	np	Perimedullary AVF type III fed by L T-6 artery; descending and ascending posterior and anterior venous drainage
5	M/18	Sudden paraplegia (18)	Increased signal of the spinal cord on proton-density and T2-weighted images	np	Perimedullary AVF type I fed by L L-1 artery; ascending posterior and anterior venous drainage
6	M/71	Paresthesias to the lower limbs, paraparesis, and urinary incontinence (70)	Increased signal of the spinal cord on proton-density and T2-weighted images	+	DAVF fed by L T-5 artery; descending and ascending anterior and posterior venous drainage
7	M/71	Hypesthesia and urinary incontinence (68)	Increased signal of the spinal cord on proton-density and T2-weighted images; perimedullary areas of signal void	np	DAVF fed by R T-12 artery; ascending anterior and posterior venous drainage
8	M/54	Low back pain, hypesthesia and paresthesias to the lower limbs, ataxia, urinary incontinence (54)	Increased signal of the spinal cord on proton-density and T2-weighted images; perimedullary areas of signal void	−	DAVF fed by L L-1 artery; ascending posterior venous drainage
9	M/70	Paraparesis, paresthesias and hypesthesia to the saddle region, and impotence (68)	Increased signal of the spinal cord on proton-density and T2-weighted images	+	DAVF fed by L T-10 artery; ascending posterior and anterior venous drainage

(*Table continues*)

Note.—AVM indicates arteriovenous malformation; AVF, arteriovenous fistula; np, not performed; DAVF, dural arteriovenous fistula; +, showed the malformation; and −, did not show the malformation.

TABLE 1: Continued

Case	Sex/Age, y	Clinical Features (age of onset, y)	MR Imaging	Myelography, CT Myelography	Selective Spinal Arteriography
10	M/75	Paraparesis, paresthesias to lower limbs and incontinence (70) recurred 8 months after embolization	Increased signal of the spinal cord on proton-density and T2-weighted images; perimedullary areas of signal void	+	DAVF fed by left T-7 artery; ascending and descending anterior and posterior venous drainage
11	M/43	Paraparesis, hypesthesia to lower limbs and incontinence (38)	Increased signal of the spinal cord on proton-density and T2-weighted images; perimedullary areas of signal void	+	DAVF fed by L L-1 and R T-12 and L-1 arteries; ascending and descending anterior and posterior venous drainage

coil was used as a receiver. In 1 patient with a cervical lesion a linearly polarized surface coil was used.

After coronal scout, sagittal 5-mm thick T1-weighted (500/30/2-4 [repetition time/echo time/excitations]) spin-echo images centered on the spinal canal were obtained with a field of view of 25 to 30 cm and a matrix of 160 × 192 or 160 × 224 pixels at the level of abnormalities shown by prior MR imaging examinations. Because there are indications that intravenous administration of paramagnetic contrast agents improves vessel conspicuity in phase contrast-MR angiography (7) (our unpublished data), gadopentetate dimeglumine (0.1 to 0.3 mmol/kg) was intravenously administered before MR angiography in all but one examination.

Details of the technical options selected for 2-D phase-contrast MR angiography of the spine are listed in Table 2. Section thickness was 30 mm in one examination and 15 to 20 mm in all the others. For sagittal MR angiography acquisitions, the field of view and matrix size were identical to those of the T1-weighted spin-echo images previously acquired. In 10 patients with thoracic lesions a 80-mm thick spatial presaturation slab was placed anteriorly to avoid ghost artifacts arising from heart motion. Care was taken not to cover the descending aorta with the presaturation slabs, because this could decrease vascular flow signal within the spinal canal. No presaturation was used in the patient with cervical lesions.

TABLE 2: Acquisition parameters for 2-D phase-contrast MR angiography of the spine

Sagittal Plane	Coronal Plane
TR = 70 ms	TR = 60 ms
TE = 27 ms	TE = 27 ms
Flip angle = 30°	Flip angle = 30°
FOV = 25 × 25 or 30 × 30 cm	FOV = 30 × 30 cm
Matrix = 160 (h) × 192 or 224 (v)	Matrix = 160 (h) × 224 (v)
Section thickness, 15 to 30 mm	Section thickness, 15 mm
VENC = 6 and 20 cm/sec	VENC = 6 and 20 cm/s
Acquisition flow directions: 3 (HF, AP, LR)	Acquisition flow directions: 3 (HF, AP, LR)
16 or 32 excitations	20 or 32 excitations
Anterior 80-mm-thick presaturation slab*	

Note.—TR indicates repetition time; TE, echo time; FOV, field of view; HF, head-feet; AP, anterior-posterior; LR, left-right; and VENC, velocity encoding.

* Not for cervical lesions.

Because the supplementary flow-encoding gradient can be inserted along only one axis (head-feet, anterior-posterior, left-right) for each acquisition, three acquisitions were needed to obtain flow information along the three axes for any plane of acquisition. In addition, amplitude and length of the bipolar gradient can be modified to detect different flow velocities optimally (6). In 10 patients velocity encoding of 6 cm/sec for low-flow vascular structures and of 15 to 20 cm/sec for high-flow vascular structures were used. This yielded a total of six acquisitions (three with velocity encoding of 6 cm/sec and 3 with velocity of 15 to 20 cm/sec) for phase-contrast MR angiography acquired in the sagittal plane and an additional six acquisitions for phase-contrast MR angiography acquired in the coronal plane. In 1 patient only sagittal acquisitions with velocity encoding of 20 cm/sec along the three flow axes were acquired.

Phase-contrast MR angiograms were reconstructed by subtraction of image pairs with inverted bipolar gradients (6). With the version of the software available, only the modulus of the phase-contrast image is reconstructed. The three modulus images representing flow along the three axes with the same velocity encoding can then be added in a total flow magnitude image.

Time needed for one phase-contrast MR angiography sequence (one flow axis with one velocity encoding) ranged between 3.12 and 5.04 minutes depending on the matrix size and the number (range, 20 to 32) of averages. Total examination time for sagittal and coronal, three flow

axes, and two different velocity encodings was about 1 hour.

Selective Spinal Arteriography

The selective spinal arteriography studies were carried out in five different centers using digital equipment in 10 patients and conventional equipment in 1. In most examinations all the spinal vascular pedicles from the vertebral to the hypogastric arteries were studied to obtain complete evaluation of spinal cord vascularization.

Data Analysis

Subtracted image pairs and total flow images of initial phase-contrast MR angiography examinations were evaluated for presence of abnormal vessels within the spinal canal. MR angiography studies were then correlated with selective spinal arteriography findings for depiction of the nidus or fistula, of the arterial feeder, and of the venous drainage. Follow-up MR angiography findings were evaluated in comparison with initial (ie, pretreatment) MR angiography findings.

Results

In sagittal low-velocity-encoded MR angiography of healthy volunteers, the anterior epidural venous plexus and the basivertebral veins were demonstrated as single longitudinal and multiple transverse, well-defined stripes behind and within the vertebral bodies. No vessel was identified directly in front of or behind the spinal cord. In coronal low-velocity-encoded MR angiography, two symmetric paramedian faint stripes were seen, possibly related to perimedullary cerebrospinal fluid flow. The anterior epidural plexus, the basivertebral veins, and perimedullary cerebrospinal fluid flow were not visible in high-velocity-encoded MR angiography.

Abnormal vessels within, in front of, or behind the spinal cord were identified with MR angiography in 10 patients (Figs 1–3). They invariably appeared as thin, sharply defined serpiginous structures. In 1 patient abnormal spinal vessels were not clearly identified.

Selective spinal arteriography revealed an intramedullary arteriovenous malformation in three patients (two of the glomus type, one of the juvenile type) (Fig 1), perimedullary arteriovenous fistula in two patients (Fig 2) (one low flow or type I and 1 of high flow or type III), and native or recurrent dural arteriovenous fistula in six patients (Fig 3).

The patient with the spinal vascular lesion missed at MR angiography had a dural arteriovenous fistula. Noteworthy is that this was the patient in whom only thick sagittal sections with high velocity encoding were obtained.

Correlation of MR angiography and selective spinal arteriography findings in 10 patients (3 with intramedullary arteriovenous malformation, 2 with perimedullary arteriovenous fistula, 5 with dural arteriovenous fistula) showed that conspicuity of the abnormal vessels within the spinal canal in high- and low-velocity-encoded phase-contrast MR angiography images was different. In fact, arterial components of intramedullary arteriovenous malformations were better seen in high-velocity-encoded images (Fig 1), whereas nidus of the arteriovenous malformations and venous drainage of intramedullary arteriovenous malformations and dural arteriovenous fistulas were better seen in low-velocity-encoded images (Figs 1 and 3). In one patient with perimedullary arteriovenous fistula the abnormal vessels were more prominent in high-flow velocity-encoded images consistent with a high-flow fistula (Fig 2), whereas in the other patient with arteriovenous fistula the abnormal vessels were better demonstrated in low-velocity-encoded images consistent with a low-flow fistula.

Sagittal MR angiography acquisitions allowed definition of the level of the nidus in intramedullary arteriovenous malformations and the anterior or posterior relationship to the spinal cord of venous drainage vessels in intramedullary arteriovenous malformations, perimedullary arteriovenous fistulas, and dural arteriovenous fistulas (Figs 1–3). However they were uninformative about the level and side of arterial feeders.

All or some of the latter were shown by coronal MR angiography acquisitions in four patients. In three patients (two with intramedullary arteriovenous malformation and one with high-flow perimedullary arteriovenous fistula) the single arterial feeder joining the abnormal vessels within the spinal canal was demonstrated in high-velocity-encoded coronal images (Fig 2). In one patient with intramedullary arteriovenous malformation of the juvenile type, one of two arterial feeders was detected in high-velocity-encoded coronal images (Fig 1) and one was missed. In three additional patients, indirect signs of the level and side of the feeders were observed. In one patient with perimedullary arteriovenous fistula, increased conspicuity of

Fig 1. Patient 3. Intramedullary arteriovenous malformation (juvenile type).

A, Sagittal T1-weighted spin-echo (500/20) MR image shows an intramedullary area of signal void corresponding to the nidus of the malformation.

B, Gadopentetate dimeglumine–enhanced phase-contrast MR angiography acquired in the sagittal plane with velocity encoding of 6 cm/s (gray scale video-reversed) shows the nidus and anterior and posterior longitudinally oriented vessels draining cranially and caudally from the nidus.

C, In gadopentetate dimeglumine–enhanced phase-contrast MR angiography acquired in the sagittal plane with velocity encoding of 20 cm/s (gray scale video-reversed), only the anterior inferior vessel is seen, consistent with high (arterial) flow velocity in its lumen.

D, Digital subtraction selective spinal arteriography (lateral projection) after catheterization of left T-5 intercostal artery (intermediate phase), shows one arterial feeder (*solid arrows*), the nidus, and a posterior descending venous drainage (*empty arrow*).

E, Gadopentetate dimeglumine–enhanced phase-contrast MR angiography acquired in the coronal plane with velocity encoding of 20 cm/s (gray scale video-reversed) demonstrates the nidus and an inferior left paramedian vessel.

F, Digital subtraction selective spinal arteriography (anterior-posterior projection) after catheterization of left T-8 intercostal artery (intermediate phase) confirms that the vessel identified in C and E is an additional arterial feeder and shows its connection with lower intercostal arteries (*arrows*).

Fig 2. Patient 4. High-flow perimedullary arteriovenous fistula (type III).

A, Sagittal T1-weighted spin-echo (500/30) MR image shows irregular hypointense areas scalloping the contours of the spinal cord.

B, Gadopentetate dimeglumine–enhanced phase-contrast MR angiography acquired in the sagittal plane with velocity encoding of 20 cm/s shows abnormal perimedullary vessels and anterior superior longitudinal vessel extending upwards for several segments (*empty arrow*).

C, Gadopentetate dimeglumine–enhanced phase-contrast MR angiography acquired in the coronal plane with velocity encoding of 20 cm/s shows the feeder of the fistula from the left T-6 intercostal artery (*arrow*) and the tangle of venous drainage in the midline below.

D, Conventional selective spinal arteriography (anterior-posterior projection) after catheterization of left T-6 intercostal artery (early phase) demonstrates hypertrophic radiculomedullary artery, which directly, without intervening nidus, drains into a perimedullary vein extending downward for several vertebral segments. The anterior superior vessel identified in B corresponded on selective spinal arteriography to an additional late-filling venous drainage of the fistula (not shown).

one intercostal artery corresponding to that of the arterial feeder was noted on low-flow velocity-encoded MR angiography (not shown). In one patient with dural arteriovenous fistula, low-velocity-encoded coronal images allowed identification of an abnormal tangle of vessels on the right side at the thoracolumbar level, which corresponded to the intradural draining vein of a fistula fed by the right T-12 intercostal artery, providing a clue about the blood supply (Fig 3). Finally, in another patient with dural arteriovenous fistula fed by the left L-1 lumbar artery, the lower extremity of the median vessel corresponding to the intradural draining vein approached the left paramedian site at the thoracolumbar junction.

Follow-up MR angiography showed persistent abnormal vessels within the spinal canal in one patient with a cervical intramedullary arteriovenous malformation who had been treated with embolization of particles 1 year before; complete occlusion of the nidus of the malformation in one patient with a thoracic intramedullary arteriovenous malformation treated with embolization of glue 6 months before; and disappearance of abnormal vessels in one patient with dural arteriovenous fistula treated with embolization of glue 3 months before.

Discussion

The potential and limitations of MR angiography in the assessment of spinal vascular malformations have to be evaluated in comparison with those of MR imaging, myelography, and CT

Fig 3. Patient 7. Spinal dural arteriovenous fistula.

A, Sagittal spin-density (1800/40) and *B,* T2-weighted (1800/100) spin-echo MR images show diffusely increased signal of the lower spinal cord, which exhibits an irregular posterior contour.

C, Sagittal T1-weighted (500/20) spin-echo MR image demonstrates scalloping of the anterior and posterior thoracic spinal cord by tiny areas of signal void.

D, Gadopentetate dimeglumine–enhanced phase-contrast MR angiography acquired in the sagittal plane with velocity encoding of 6 cm/s demonstrates prominent abnormal vessels in front of and behind the thoracic spinal cord.

E, Gadopentetate dimeglumine–enhanced phase-contrast MR angiography acquired in the coronal plane with velocity encoding of 6 cm/s shows irregular serpiginous structure in the midline and a tangle of vessels in the right paramedian site at the thoracolumbar junction.

F, Digital subtraction selective spinal arteriography (anterior-posterior projection) after catheterization of right T-12 intercostal artery (intermediate phase) shows the fistula (*arrow*) and the intradural draining vein, which exhibits a tortuous course. Note the resemblance between the shape of the proximal segment of the intradural draining vein in E and F.

after myelography on one hand and selective spinal arteriography on the other (1, 8). MR imaging in spinal vascular malformations shows intramedullary and perimedullary serpiginous structures of signal void on spin-echo images (1, 8–13). These are sometimes associated with intramedullary signal changes related to hemorrhage or ischemia of the spinal cord (1, 8–13). The latter features are nonspecific and differential diagnosis with other conditions can be extremely difficult if intramedullary or perimedullary vessels are not seen. Conversely, false-positive MR findings can occur because of cerebrospinal fluid flow phenomena (8). These reasons justify the use of myelography and CT myelography after inconclusive MR imaging examinations in screening for spinal vascular malformations.

Our results indicate that MR angiography may help to detect intramedullary or perimedullary vessels that are occult or barely detectable by conventional MR imaging.

It is noteworthy that incomplete or inappropriate technical choices in terms of velocity encoding and section thickness were made in the study of the only vascular malformation missed at MR angiography in our series.

Based on our results, we cannot answer the question of whether MR imaging with MR angiography can now replace myelography in screening for spinal vascular malformations. Notable in this respect are two patients in our series. One (number 8) had false-negative myelography and CT myelography with MR imaging and angiography positive for abnormal vessels within the spinal canal. The other (number 9) had positive myelography but MR imaging and angiography were false-negative for abnormal vessels within the spinal canal. More case series comparing MR imaging plus angiography with myelography are needed to resolve this important issue.

As mentioned, classification of spinal vascular malformations and identification of the number, level, and side of the arterial feeders as well as depiction of the venous drainage are usually not possible with MR imaging or myelography and require selective spinal arteriography.

Admittedly, at this stage of its development MR angiography cannot substitute for selective spinal arteriography for these purposes. However, our results suggest that MR angiography may sometimes help selective spinal arteriography planning. In fact MR angiography showed the nidus in all three patients with intramedullary arteriovenous malformations and allowed the direct or indirect identification of the side and the level of at least one arterial feeder in all five patients with intramedullary arteriovenous malformation or perimedullary arteriovenous fistula.

The poor demonstration at MR angiography of the arterial feeder and fistula in all our patients with dural arteriovenous fistula is not surprising because these structures are usually of very small size, and the fistula itself is sometimes not seen even on selective spinal arteriography (1). The side and level of the fistula could, however, be suspected because of the shape of the intradural draining vein identified with coronal MR angiography in two of six patients with dural arteriovenous fistula.

Finally our results, although limited to three patients, suggest that MR angiography in conjunction with MR imaging can be used in the follow-up of patients with spinal vascular malformations after treatment.

Because of more efficient background suppression and less vulnerability to saturation phenomena, we and other authors chose phase contrast rather than time-of-flight technique for MR angiography of spinal vascular lesions (2, 14; Mascalchi M et al, "Phase-Contrast versus Time-of-Flight MRA of Spinal Vascular Malformations," presented at the Twelfth Annual Meeting of the Society of Magnetic Resonance in Medicine, Berkeley, Calif, 1993).

Several technical limitations of our study have to be considered. First, the study was carried out on a midfield MR unit, implying a relatively low signal-to-noise ratio. This was partially balanced by increasing the number of averages for each acquisition at the expense of the total examination time. Second, because of hardware constraints, 3-D (volume) gradient-echo sequences for MR angiography were not available. Such sequences allow thinner sections with higher spatial resolution and reduced flow-related dephasing effects because of the smaller voxel size (14). An additional technical limitation in our study was the relatively long minimum echo time for flow-encoded gradient-echo sequences resulting in increased risk for ghost artifacts and reduced signal because of dephasing (6, 7). Finally, with the coils used we were forced to reduce the size of the field of view in order to obtain satisfactory spatial resolution. This limitation unavoidably restricts the panorama of the MR angiography images. Availability of multiarray coils, which enable high-resolution images with large fields of view (15), should improve the panorama of MR angiography examination in the future.

Notwithstanding the above difficulties, the overall depiction of the spinal vascular anomalies in our series was satisfactory and to some extent surprising.

In conclusion, our results indicate that MR angiography with 2-D phase-contrast technique complements conventional MR imaging in the evaluation of spinal vascular malformations by improving the confidence or detection of abnormal vessels within the spinal canal. In addition, in some patients it may provide useful information for selective spinal arteriography planning concerning the level and the side of the vascular

pedicles feeding the malformation. Finally, MR angiography is possibly an important noninvasive tool for monitoring the results of treatment.

References

1. Berenstein A, Lasjaunias P. Endovascular treatment of spine and spinal cord lesions. *Surgical Neuro-angiography. Vol V.* Berlin; Springer-Verlag 1992:1–85
2. Gelbert F, Guichard JP, Mourier KL et al. Phase-contrast MR angiography of vascular malformations of the spinal cord at 0.5 T. *J Magn Reson Imaging* 1992;2:631–636
3. Ruggieri PM, Masaryk TJ, Ross JS, Modic MT. Intracranial magnetic resonance angiography. *Cardiovasc Intervent Radiol* 1992; 15:71–81
4. Bowen BC, Kochan JP, Margosina P, Quencer RM, Donovan-Post MJ, Green BA. Time of flight MR angiography of spinal vascular abnormalities. *Radiology* 1992;185(P):122
5. Mourier KL, Gelbert F, Reizine D et al. Phase-contrast magnetic resonance of the spinal cord arteriovenous malformations. *Acta Neurochir* 1993;123:57–63
6. Dumoulin CL, Hart HR Jr. Magnetic resonance angiography. *Radiology* 1986;161:717–720
7. Tu R, Kennel T, Turski P, Polzin J, Korosec F. Mistretta C. Preliminary assessment of gadodiamide-enhanced, complex difference phase-contrast magnetic resonance angiography. *Acad Radiol* 1994;S47–S55
8. Enzmann DR. Vascular diseases. In: Enzmann DR, DeLaPaz RL, Rubin JB, eds. *Magnetic Resonance of the Spine* St Louis: C V Mosby Co; 1990:533–539
9. Di Chiro G, Doppman JL, Dwyer AJ, et al. Tumors and arteriovenous malformations of the spinal cord: assessment using MR. *Radiology* 1985;156:689–697
10. Minami S, Sagoh T, Nishimura K, et al. Spinal arteriovenous malformations: MR imaging. *Radiology* 1988;169:109–115
11. Dormont D, Gelbert F, Assouline E, et al. MR imaging of spinal cord arteriovenous malformations at 0.5 T: study of 34 cases. *AJNR Am J Neuroradiol* 1988;9:833–838
12. Masaryk TJ, Ross JS, Modic MT, et al. Radiculomeningeal vascular malformations of the spine: MR imaging. *Radiology* 1987; 164:845–849
13. Larrson EM, Desai P, Hardin CW, Story, Jinkins JR. Venous infarction of the spinal cord resulting from dural arteriovenous fistula: MR imaging findings. *AJNR Am J Neuroradiol* 1991;12: 739–743
14. Edelman RR. Basic principles of magnetic resonance angiography. *Cardiovasc Intervent Radiol* 1992;15:3–13
15. Roemer PB, Edelstein WA, Hayes CE, Souza SP, Mueller OM. The NMR phased array. *Magn Reson Med* 1990;15:192–225

А

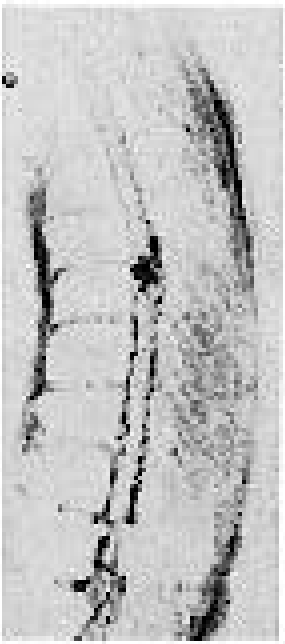

Б

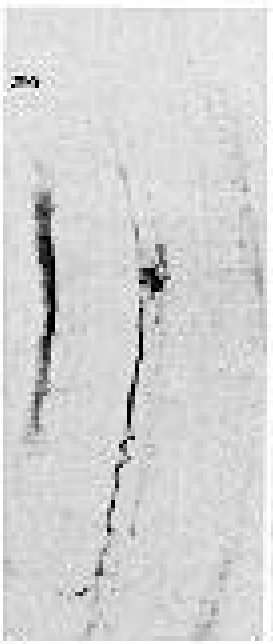

В

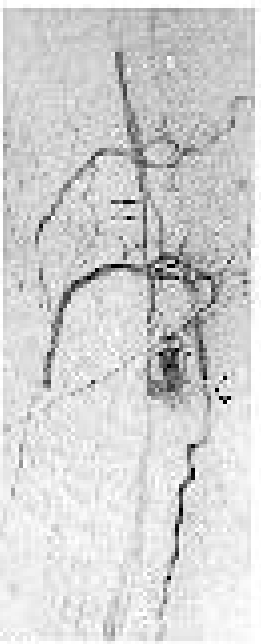

Д

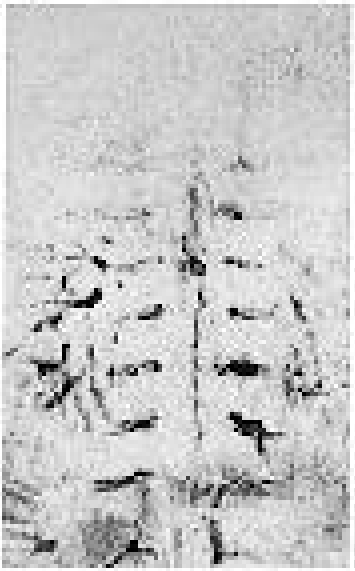

Г

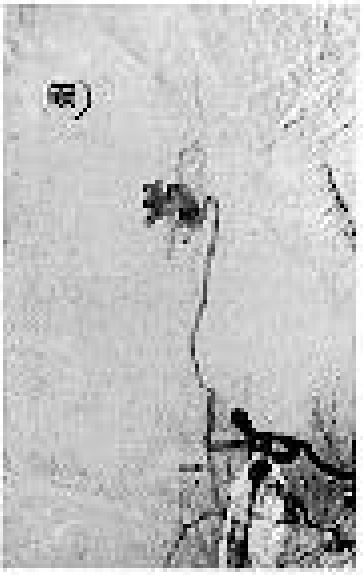

Г

A

B

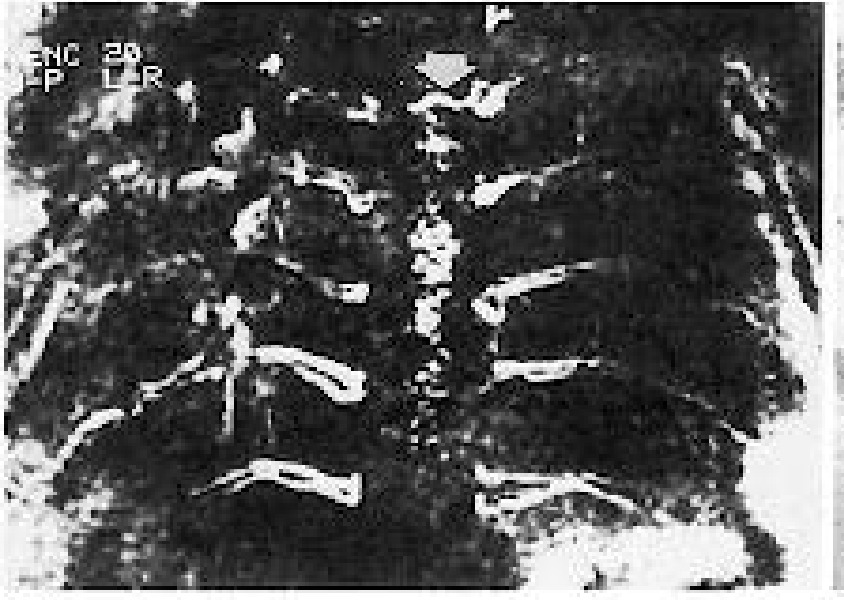

C

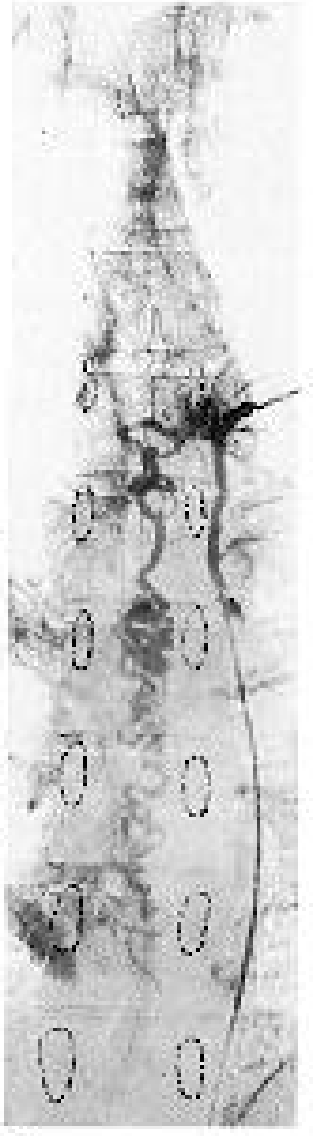

D


A
B
C
D

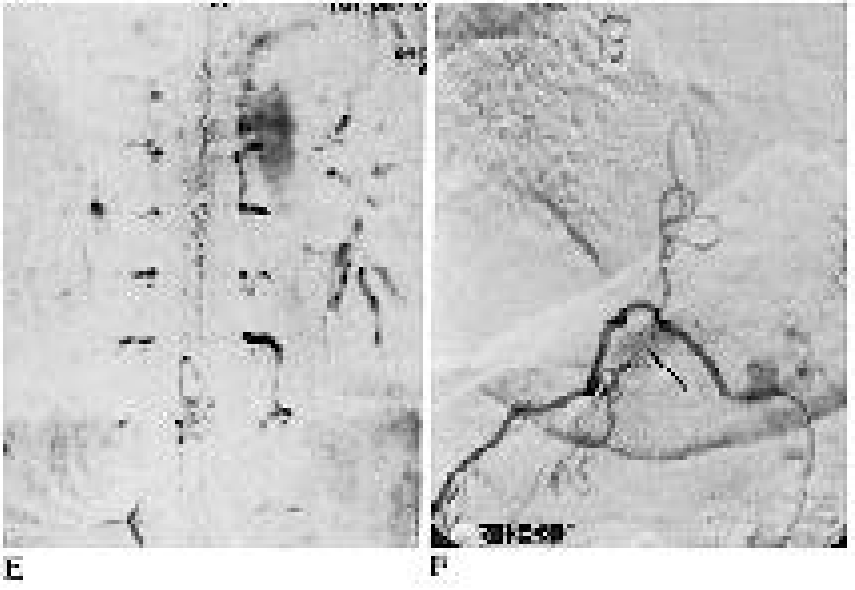
E
F